



## Special Feature: Power Semiconductor Devices

Research Report

### Evaluation of Dry Etching-induced Damage in p-type GaN by Hard X-ray Photoelectron Spectroscopy

Daigo Kikuta, Tetsuo Narita, Naoko Takahashi, Keita Kataoka, Yasuji Kimoto, Kazuyoshi Tomita, Tsutomu Uesugi, Tetsu Kachi and Masahiro Sugimoto

Report received on Aug. 24, 2015

**■ABSTRACT■** Dry etching-induced damage in p-type GaN was investigated using hard X-ray photoelectron spectroscopy (HAXPES). An analytical expression for the Ga  $2p_{3/2}$  spectrum was developed, which reflects the band bending. The calculated spectra were consistent with the experimental spectra, including consideration of the take-off angle. The analysis was extended to deal with dry etching-induced damage and the deep donor concentration induced by dry etching was successfully evaluated.

The effect of post-etching processes was also investigated for dry-etched p-type GaN using HAXPES. The analysis results reveal the presence of surface deep donor layers due to etching-induced damage, and the parameters of the surface band diagram were determined. The as-etched sample has a deep donor concentration of  $2.8 \times 10^{19} \text{ cm}^{-3}$ . The built-in potential of the as-etched sample was estimated to be 1.14 eV. Exposure to  $\text{O}_2$  plasma with subsequent HF treatment resulted in the lowest built-in potential ( $V_{\text{bi}}$ ) of 0.65 eV and the smallest damage layer thickness ( $W_{\text{damage}}$ ) of 5.4 nm, although the  $V_{\text{bi}}$  and  $W_{\text{damage}}$  values for the sample exposed to only  $\text{O}_2$  plasma without subsequent HF treatment were 0.86 eV and 5.7 nm, respectively. Therefore, HF treatment plays a key role in the reduction of  $V_{\text{bi}}$  and the  $W_{\text{damage}}$ .

**■KEYWORDS■** Hard X-ray Photoelectron Spectroscopy (HAXPES), GaN, Band Diagram, Dry Etching-induced Damage, Deep Donor, Build-in Potential,  $\text{O}_2$  Plasma, HF Treatment

#### 1. Introduction

Gallium nitride (GaN) is a promising semiconductor material for switching devices, which have attracted significant attention as power devices for high-efficiency inverters and converters.<sup>(1)</sup> High-efficiency inverters and converters are in strong demand for hybrid, electric and fuel-cell vehicles, which have many electrical power conversion units in their systems, to improve the fuel efficiency.

GaN-based power devices are commonly fabricated using dry etching processes. However, degradation of the electrical characteristics caused by this process, such as poor ohmic contact to dry-etched p-type GaN due to etching-induced damage near the surface, is a serious problem.<sup>(2)</sup> The etching-induced damage causes an energy barrier for hole transport due to surface band bending. Therefore, a more detailed understanding of etching-induced damage and surface band bending is expected to accelerate improvement of the ohmic contact for p-type GaN and the development of GaN power devices.

Dry etching-induced damage is commonly evaluated using deep level transient spectroscopy (DLTS) or measurement of the ideality factor and barrier height of Schottky diodes. However, these methods require metal contact formation processes, which could lead to changes in the properties of the etching-induced damage.

Hard X-ray photoelectron spectroscopy (HAXPES) is a non-destructive technique used to investigate the electronic structures and chemical states of near-surface regions (typically 10 nm in depth) due to the high kinetic energy of the photoelectrons involved.<sup>(3)</sup> In this study, HAXPES was applied to evaluate etching-induced damage of dry-etched p-type GaN. Quantitative analysis of surface band bending in the depth direction was also conducted. Furthermore, the effect of the post-etching processes on dry-etched p-type GaN was investigated by surface band bending analysis.

## 2. Modification of the Photoelectron Spectrum by Surface Band Bending

We first discuss the modification of the photoelectron spectrum by surface band bending. **Figure 1** shows a schematic image of band bending in p-type GaN. Surface states or surface defects cause the Fermi energy of the surface to be pinned. Holes are depleted by a built-in potential ( $V_{bi}$ ) and band bending occurs toward the surface.

Assuming that the concentration of acceptors is uniform, the potential in the depletion region ( $V_{dep}$ ) is expressed by:

$$V_{dep} = -\frac{qN_A}{2\epsilon_s}(x - x_D)^2. \quad (1)$$

$q$ : electron charge

$N_A$ : concentration of acceptors

$\epsilon_s$ : permittivity of the semiconductor

$x$ : depth from the surface

$x_D$ : depth of the depletion region

The binding energy of Ga  $2p_{3/2}$  with respect to the Fermi level in the depletion region ( $E_{Ga2p3/2\_dep}$ ) is the sum of the binding energy of Ga  $2p_{3/2}$  in the bulk region ( $E_{Ga2p3/2\_bulk}$ ) and  $V_{dep}$ . Therefore,  $E_{Ga2p3/2\_dep}$  is given by:

$$E_{Ga2p3/2\_dep} = E_{Ga2p3/2\_bulk} + V_{dep}. \quad (2)$$

The probe depth of HAXPES is characterized by the photoelectron escape depth, which is related to the inelastic mean-free path (IMFP) of a photoelectron and its take-off angle. The IMFP of photoelectrons

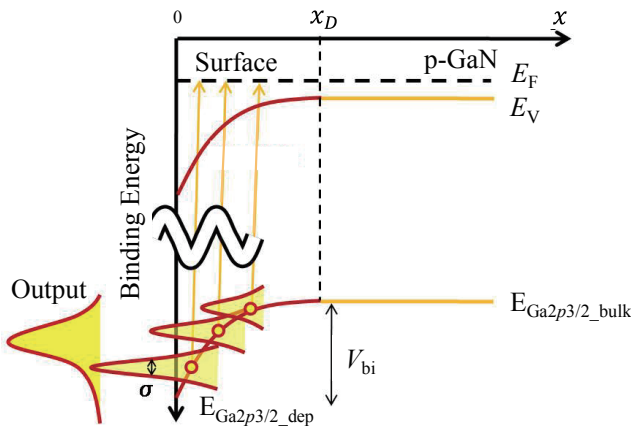


**Fig. 1** Schematic image of band bending in p-type GaN.

from Ga  $2p_{3/2}$  is 9.0 nm, and the escape depth is estimated to be 8.8 nm for take-off angles of  $80^\circ$  using the TTP2M formula.<sup>(4)</sup> The probe depth is sufficiently larger than the distribution of  $E_{Ga2p3/2\_dep}$ ; therefore,  $E_{Ga2p3/2\_dep}$  varies with the probe depth. The spectrum of Ga  $2p_{3/2}$  measured using HAXPES therefore includes information on the potential distribution of the depletion region.

The formula for the Ga  $2p_{3/2}$  spectrum that reflects the band bending,  $F_{Ga2p3/2}(E)$ , can be expressed as:

$$F_{Ga2p3/2}(E) = \int_0^\infty \left[ \exp(-x/\lambda) \times \exp\left(-\frac{(E - E_{Ga2p3/2\_dep}(x))^2}{2\sigma^2}\right) \right] dx. \quad (3)$$

$\lambda$ : photoelectron escape depth

$E$ : photon energy

$\sigma$ : standard deviation of the Ga  $2p_{3/2}$  photoelectron energy

In this formula, it is assumed that the spectrum can be expressed by the convolution of Gaussian-shaped spectra over all depths. This indicates that band-bending and the concentration of acceptors in p-type GaN can be estimated using HAXPES.

To confirm the performance of the Eq. (3), the Ga  $2p_{3/2}$  spectrum for a p-type GaN was measured using HAXPES and compared with the calculated spectrum. Samples for HAXPES measurements were prepared as follows. First, p-type GaN films were deposited by conventional metalorganic chemical vapor deposition onto sapphire substrates. Magnesium ions were doped in the films as acceptors at a concentration of  $2.5 \times 10^{19} \text{ cm}^{-3}$ . The films were annealed at  $850^\circ \text{C}$  in  $\text{N}_2$  for 5 min to activate the Mg. HAXPES measurements were conducted at the BL46XU beamline of SPring-8 using an incident photon energy of 7942.6 eV.

**Figure 2** shows the measured Ga  $2p_{3/2}$  spectra for various take-off angles. The peak-top energy of the Ga  $2p_{3/2}$  spectrum with a take-off angle of  $12^\circ$  was the highest of all the take-off angles examined. The probe depth decreased with the take-off angle, so that the Ga  $2p_{3/2}$  spectrum was more affected by  $V_{dep}$ . Therefore, a higher binding energy is obtained from a spectrum measured with a lower take-off angle.

Figure 2 also shows the calculated Ga  $2p_{3/2}$  spectra.  $N_A$  and  $V_{bi}$  were assumed to be  $4.3 \times 10^{19} \text{ cm}^{-3}$  and 1.8 eV, respectively. The calculated spectra are in good agreement with the experimental results. The  $V_{bi}$  of

1.8 eV corresponds fairly well with the value of 1.6 eV reported by Hashizume.<sup>(5)</sup> These results indicate that  $N_A$  and  $V_{bi}$  related to the surface band bending can be estimated using HAXPES.

### 3. Estimation of Defect Concentration in Dry-etched p-type GaN

In Section 2, it was indicated that the acceptor concentration can be estimated from the Ga  $2p_{3/2}$  spectra. Dry-etched p-type GaN contains shallow acceptors and deep donors, which are induced by dry etching near the surface.  $V_{dep}$  is essentially a function of the concentration of net ionized impurities. The concentration of net-ionized impurities ( $N_{net}$ ) is expressed as:

$$N_{net} = N_{SD} + N_{DD} - N_{SA} - N_{DA}. \quad (4)$$

$N_{SD}$ : concentration of shallow donors  
 $N_{DD}$ : concentration of deep donors  
 $N_{SA}$ : concentration of shallow acceptors  
 $N_{DA}$ : concentration of deep acceptors

$N_{SD}$  and  $N_{DA}$  are very small and can be ignored in p-type GaN. Therefore, Eq. (1) can be rewritten as:

$$V_{dep} = -\frac{q(N_{SA} - N_{DD})}{2\epsilon_s} (x - x_D)^2. \quad (5)$$

If  $N_{SA}$  has already been obtained, then  $N_{DD}$  can be estimated from the Ga  $2p_{3/2}$  spectrum.

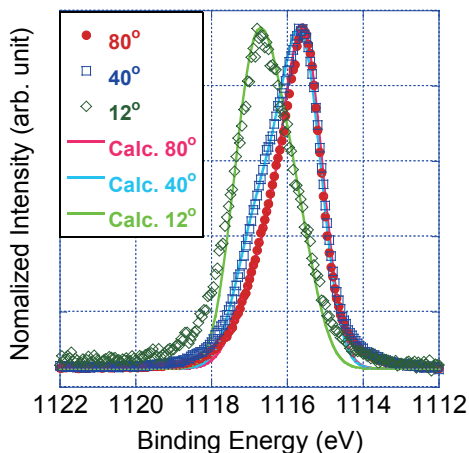


**Fig. 2** HAXPES Ga  $2p_{3/2}$  spectra with take-off angles of 80°, 40° and 12°. Symbols and solid lines represent experimental and calculated data, respectively.

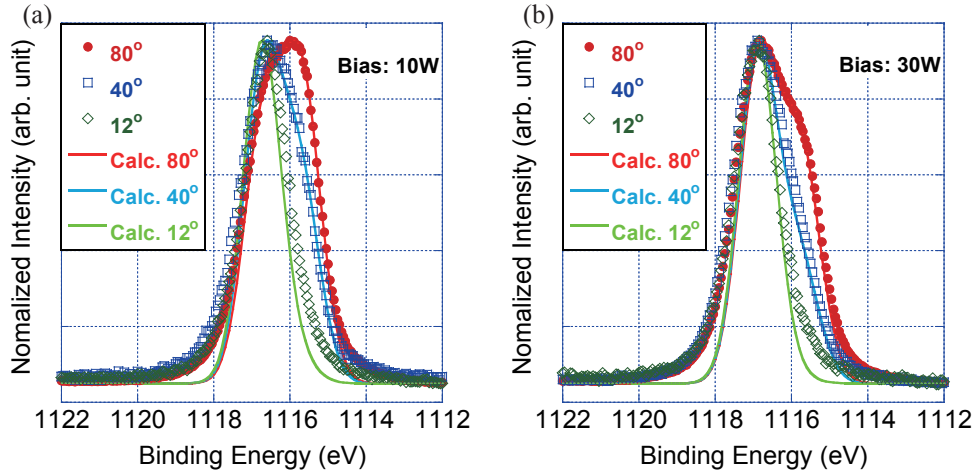
**Figure 3** shows experimental Ga  $2p_{3/2}$  spectra for dry-etched p-type GaN films, which were prepared in the same manner as those discussed in Section 2, followed by dry etching with  $Cl_2$ -based inductively-coupled plasma.  $Cl_2$  and  $BCl_3$  were used as etching gases at flow rates of 25 and 5 sccm, respectively. The etching pressure and antenna power were 1 Pa and 300 W, respectively. Bias powers of 10 W and 30 W were utilized. The details for sample preparation have been previously reported in Ref. (6).

Figure 3 also shows the calculated Ga  $2p_{3/2}$  spectra.  $N_{SA}$  was assumed to be  $4.3 \times 10^{19} \text{ cm}^{-3}$ . A constant concentration of deep donors in the depth direction and an abrupt doping profile were also assumed. The calculated spectra correspond well with the experimental results. The thickness of the damage layers ( $W_{damage}$ ) with bias power of 10 W and 30 W were estimated to be 5 and 8 nm, respectively. Thus,  $W_{damage}$  increased with the bias power. The  $N_{DDs}$  values in p-type GaN, dry etched with bias powers of 10 W and 30 W, were estimated to be greater than  $1 \times 10^{20} \text{ cm}^{-3}$ .

**Figure 4** shows a schematic image of the obtained band diagrams. Dry etching-induced damage can thus be successfully evaluated using HAXPES, and the band diagram can be produced from the obtained values.

### 4. Effect of Post-processes for Dry-etched p-type GaN

In Section 3, it was demonstrated that damage due to dry-etching can be evaluated using HAXPES. Additionally, this evaluation technique was also used to investigate the effects of post-processes on dry-etched p-type GaN. Samples were prepared in the same manner as described in the previous sections, and the etching conditions were the same as those described in Section 3. The following post-etching processes were examined. Sample A was annealed at 850 °C in  $N_2$  for 5 min. Sample B was annealed at 600 °C in  $O_2$  for 3 min. Sample C was exposed to  $O_2$  remote plasma for 2 min. As-etched (Sample D) and as-grown (Sample E) samples were also prepared as references. These samples were treated with a standard RCA clean, followed by immersion in 25% hydrofluoric acid (HF) to remove the surface oxidized layers. To investigate the effect of the HF treatment, sample C' was prepared without HF treatment. **Figure 5** shows a flow chart of the preparation sequences, the details of which have



**Fig. 3** HAXPES Ga  $2p_{3/2}$  spectra for dry-etched p-type GaN with a bias power of (a) 10 W and (b) 30 W. Symbols and solid lines represent experimental and calculated data, respectively.

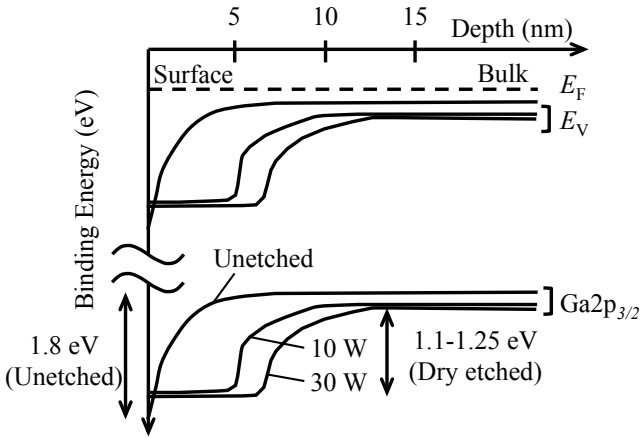


**Fig. 4** Simulated band diagram using obtained parameters from the HAXPES analysis.

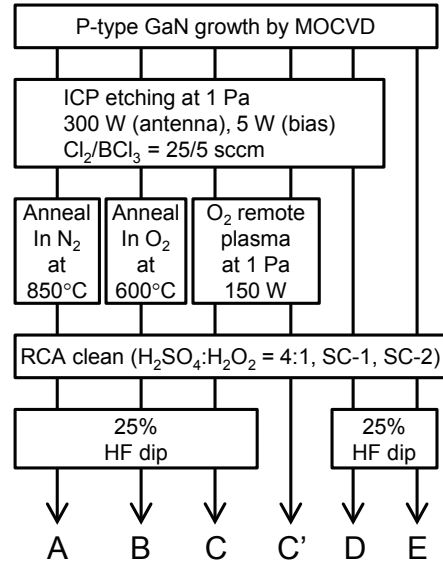


**Fig. 5** The flowchart of sample preparation.

been reported in Ref. (7). HAXPES measurements were conducted at the BL46XU beamline of SPring-8 under the same conditions as those described in Section 2. In this experiment, we decided to measure N1s photoelectron spectra rather than Ga  $2p_{3/2}$  spectra because the former provided higher energy resolution.

**Figure 6** shows the measured spectra. For sample E, the data fitting was performed using Eq. (3). The calculated data are shown as solid lines in Fig. 6(e).  $N_A$  and  $V_{bi}$  were estimated to be  $2.7 \times 10^{19} \text{ cm}^{-3}$  and 1.43 eV, respectively. For dry-etched samples, it was assumed there was an abrupt junction between the p-type layer and the damaged layer that contained the acceptors and deep donors due to dry-etching damage.

Calculations for the dry-etched samples are also shown in Figs. 6(a)-(d).  $W_{\text{damage}}$  and  $V_{bi}$  near the surface, as well as  $N_{DD}$  and  $N_{SA}$  were determined from the fitting results. The obtained parameters are summarized in **Table 1**.

$V_{bi}$  for the as-grown sample was higher than that for the as-etched sample. Hashizume reported that excess Mg and oxides introduced high-density surface states on the p-GaN surface, which led to strong Fermi level pinning around 1.6 eV above the valance band maximum at the surface.<sup>(5)</sup> Therefore, the removal of excess Mg and oxides by dry etching could cause the

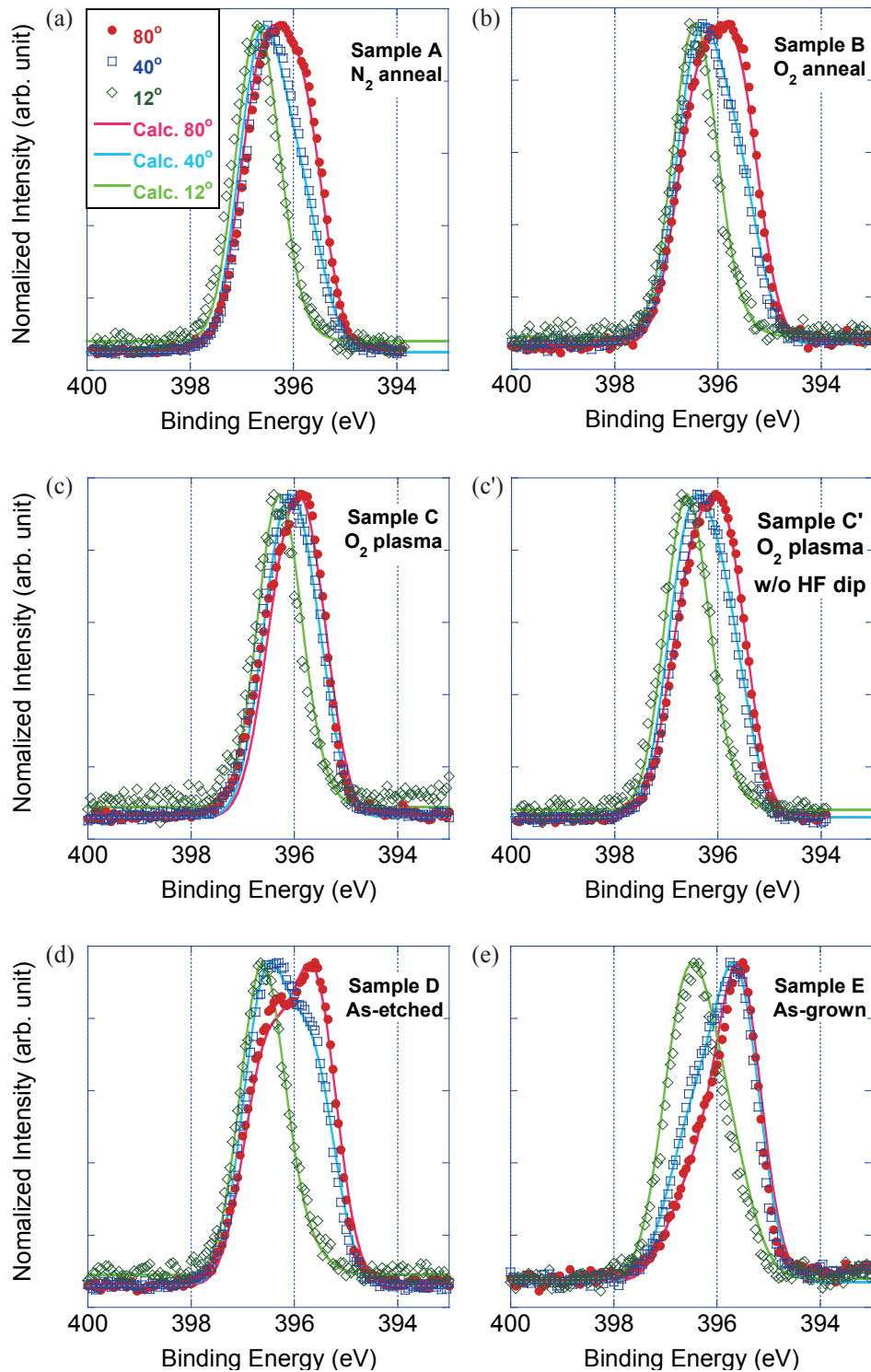


**Fig. 6** HAXPES N1s spectra for p-type GaN; (a) annealed in N<sub>2</sub>, (b) annealed in O<sub>2</sub>, (c) exposed to O<sub>2</sub> plasma with subsequent HF treatment, (c') exposed to O<sub>2</sub> plasma without HF treatment, (d) as-etched, and (e) as-grown. Symbols and solid lines represent experimental and calculated data, respectively.

smaller  $V_{bi}$  of the as-etched sample.

$V_{bi}$  for the samples annealed in N<sub>2</sub> and O<sub>2</sub> atmospheres were smaller than that for the as-etched sample.

However,  $W_{\text{damage}}$  for the samples annealed in N<sub>2</sub> and O<sub>2</sub> atmospheres were larger than that for the as-etched sample. These results indicate the formation of donor

**Table 1** Parameters of surface band bending obtained by HAX-PES analyses.

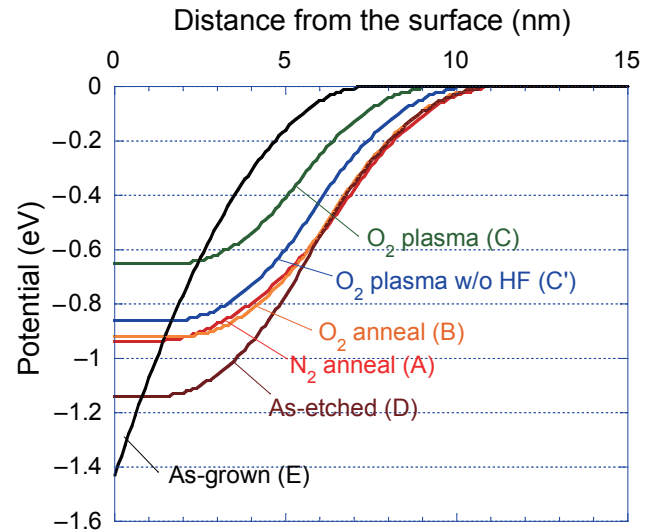
Parameter	Sample A N <sub>2</sub> anneal	Sample B O <sub>2</sub> anneal	Sample C O <sub>2</sub> plasma	Sample C' O <sub>2</sub> plasma w/o HF dip	Sample D As-etched	Sample E As-grown
$W_{\text{damage}}$ (nm)	6.9	6.3	5.4	5.7	5.6	-
$V_{\text{bi}}$ (eV)	0.94	0.92	0.65	0.86	1.14	1.43
$N_{\text{DD}}$ (cm <sup>-3</sup> )	$1.6 \times 10^{19}$	$2.4 \times 10^{19}$	$2.5 \times 10^{19}$	$2.5 \times 10^{19}$	$2.8 \times 10^{19}$	-
$N_{\text{SA}}$ (cm <sup>-3</sup> )	$2.2 \times 10^{19}$	$2.2 \times 10^{19}$	$2.2 \times 10^{19}$	$2.2 \times 10^{19}$	$2.2 \times 10^{19}$	$2.7 \times 10^{19}$

states and the diffusion of donor states to the p-type layer. Relatively low migration barriers for nitrogen vacancies have been reported and the mechanism for the formation of complexes between nitrogen vacancies and more stable defects during annealing was reported.<sup>(8,9)</sup> Therefore, annealing as a post-etching process may lead to the formation of different defect states, such as nitrogen vacancy complexes that result in different  $V_{\text{bi}}$ .

The  $V_{\text{bi}}$  for sample C' (exposed to O<sub>2</sub> plasma without subsequent HF treatment) was 0.86 eV, which indicates that deep donors with an energy level of approximately 0.8 eV from the valance band maximum were formed near the surface due to O<sub>2</sub> plasma exposure. The concentration of deep donors in sample C' was estimated from the fitting results to be  $2.5 \times 10^{19}$  cm<sup>-3</sup> and  $W_{\text{damage}}$  was estimated to be 5.7 nm.

$V_{\text{bi}}$  and  $W_{\text{damage}}$  for sample C (exposed to O<sub>2</sub> plasma with subsequent HF treatment) were estimated to be 0.65 eV and 5.4 nm, respectively, which indicates that HF treatment is effective to reduce  $V_{\text{bi}}$  and  $W_{\text{damage}}$ . Lee et al. reported that surface oxides on p-type GaN cause a positive electric field due to trapped holes in the surface oxides; the surface oxide thus forms higher built-in potentials.<sup>(10)</sup> The smaller  $V_{\text{bi}}$  and  $W_{\text{damage}}$  values for the sample exposed to O<sub>2</sub> plasma with subsequent HF treatment may be due to removal of the surface oxide.

**Figure 7** shows the simulated energy band diagram constructed using the parameters in Table 1. The annealing processes were effective in reducing  $V_{\text{bi}}$ , where the most effective process to reduce both  $V_{\text{bi}}$  and  $W_{\text{damage}}$  was exposure to O<sub>2</sub> plasma with subsequent HF treatment.

**Fig. 7** Calculated band diagrams using the parameters obtained from the HAXPES analyses.

## 5. Conclusion

Dry etching-induced damage in p-type GaN was investigated using HAXPES. First, an expression for the Ga 2p<sub>3/2</sub> photoelectron spectrum that reflects band bending was developed. The calculated spectra corresponded well with the experimental spectra, including consideration of the take-off angle. The formula was extended to deal with dry etching-induced damage, whereby the deep donors induced by dry etching could be successfully evaluated.

Second, the effect of post-etching processes was investigated using the developed analysis method.  $V_{\text{bi}}$  for the as-etched sample was estimated to be

1.14 eV, whereas  $V_{bi}$  for the samples annealed in  $N_2$  or  $O_2$  atmospheres were reduced to 0.94 and 0.92 eV, respectively. Exposure to  $O_2$  plasma with subsequent HF treatment gave the lowest  $V_{bi}$  of 0.65 eV, although  $V_{bi}$  for the sample exposed to  $O_2$  plasma without subsequent HF treatment was 0.86 eV.  $W_{damage}$  for the sample exposed to  $O_2$  plasma with subsequent HF treatment was smaller than that without subsequent HF treatment. Thus, HF treatment may remove surface oxide and thereby play a key role in reducing the potential barrier and damage layer thickness.

### Acknowledgements

The synchrotron radiation experiments were performed at the BL46XU beamline of SPring-8 with the approval of the Japan Synchrotron Radiation Research Institute (JASRI) (Proposal Nos. 2009B2008, 2010A1805, 2010B1915). The authors thank Dr. Machida, Dr. Sun and Dr. Oji of JASRI for their support.

### References

- (1) Sugimoto, M., Ueda, H., Uesugi, T. and Kachi, T., *Proc. of the 2006 Lester Eastman Conf.* (2006), pp. 3-9, World Scientific Pub. Co. Pte. Ltd.
- (2) Lin, Y. J. and Chu, Y. L., *J. Appl. Phys.*, Vol. 97, No. 10 (2005), 104904.
- (3) Toyoshima, Y., Horiba, K., Oshima, M., Ohta, J., Fujioka, H., Miki, H., Ueda, S., Yamashita, Y., Yoshikawa, H. and Kobayashi, K., *Appl. Surf. Sci.*, Vol. 255, No. 5 (2008), pp. 2149-2152.
- (4) Tanuma, S., Powell, C. J. and Penn, D. R., *Surface and Interface Analysis*, Vol. 21, No. 3 (1994), pp. 165-176.
- (5) Hashizume, T., *J. Appl. Phys.*, Vol. 94, No. 1 (2003), pp. 431-436.
- (6) Narita, T., Kikuta D., Takahashi, N., Kataoka, K., Kimoto, Y., Uesugi, T., Kachi, T. and Sugimoto, M., *Phys. Status Solidi A*, Vol. 208, No. 7 (2011), pp. 1541-1544.
- (7) Kikuta, D., Narita, T., Takahashi, N., Kataoka, K., Kimoto, Y., Tomita, K., Uesugi, T. and Kachi, T., *Phys. Status Solidi C*, Vol. 9, No. 3-4 (2012), pp. 927-930.
- (8) Limpijumnong, S. and Van de Walle, C. G., *Phys. Rev. B*, Vol. 69, No. 3 (2004), 035207.
- (9) Reshchikov, M. A. and Morkoç, H., *J. Appl. Phys.*, Vol. 97, No. 6 (2005), 061301.
- (10) Lee, J. L., Weber, M., Kim, J. K., Lee, J. W., Park, Y. J., Kim, T. and Lynn, K., *Appl. Phys. Lett.*, Vol. 74, No. 16 (1999), pp. 2289-2291.

Figs. 1-4

Reprinted and modified from *Phys. Status Solidi A*, Vol. 208, No. 7 (2011), pp. 1541-1544, Narita, T., Kikuta, D., Takahashi, N., Kataoka, K., Kimoto, Y., Uesugi, T., Kachi, T. and Sugimoto, M., *Study of Etching-induced Damage in GaN by Hard X-ray Photoelectron Spectroscopy*, © 2011 John Wiley & Sons, Ltd., with permission from John Wiley & Sons, Ltd.

Figs. 5-7 and Table 1

Reprinted and modified from *Phys. Status Solidi C*, Vol. 9, No. 3-4 (2012), pp. 927-930, Kikuta, D., Narita, T., Takahashi, N., Kataoka, K., Kimoto, Y., Tomita, K., Uesugi, T. and Kachi, T., *Study on Post-etching Processes for p-type GaN Using HAX-PES*, © 2012 John Wiley & Sons, Ltd., with permission from John Wiley & Sons, Ltd.

### Daigo Kikuta

Research Fields:

- GaN-based Power Devices: Fabrication Process
- Device Characterization

Academic Degree: Dr.Eng.

Academic Societies:

- The Japan Society of Applied Physics
- The Institute of Electronics, Information and Communication Engineers



### Tetsuo Narita

Research Field:

- III-Nitride Semiconductor: Growth, Power Device and Physics

Academic Degree: Dr.Eng.

Academic Society:

- The Japan Society of Applied Physics



### Naoko Takahashi

Research Fields:

- Surface Analysis
- Synchrotron Radiation Analysis

Academic Societies:

- Japanese Society of Tribologist
- The Japan Society of Applied Physics
- The Surface Science Society of Japan



### Keita Kataoka

Research Fields:

- Semiconductor Physics
- Surface and Interface Analysis

Academic Degree: Dr.Sci.



---

**Yasuji Kimoto**

Research Field:

- Surface Analysis

Academic Society:

- The Japan Society of Applied Physics



---

**Kazuyoshi Tomita**

Research Field:

- GaN Power Devices

Academic Degree: Dr.Eng.

Academic Society:

- The Japan Society of Applied Physics



---

**Tsutomu Uesugi**

Research Fields:

- Power Devices
- Compound Semiconductor

Academic Degree: Ph.D.

Academic Societies:

- The Japan Society of Applied Physics
- The Institute of Electrical Engineers of Japan
- IEEE

Award:

- 30th JSAP Outstanding Paper Award, The Japan Society of Applied Physics, 2008



---

**Tetsu Kachi**

Research Field:

- Power Electronics and Power Devices

Academic Degree: Dr.Eng.

Academic Societies:

- The Japan Society of Applied Physics
- The Institute of Electronics, Information and Communication Engineers

Award:

- 30th JSAP Outstanding Paper Award, The Japan Society of Applied Physics, 2008



---

**Masahiro Sugimoto\***

Research Field:

- SiC-based Power Devices: Device Characterization

Academic Society:

- The Japan Society of Applied Physics



---

\* Toyota Motor Corporation